EUROPEAN FUSION DEVELOPMENT AGREEMENT

EFDA–JET–CP(01)02-97

M.N.A.Beurskens, E.Giovannozzi, J.Gunn, Y.Andrew, M.Brix, J-MChareau, K.Erents, C.Gowers, K.Günther, S.Jachmich, A.Kallenbach, A.Korotkov, E. de la Luna, P.Morgan, R.Prentice, M.Proschek, G.Saibene, W.Suttrop, J-MTravere, V.Tribaldos, M.Zerbini and JET EFDA Contributors

Analysis of Plasma EDGE Profiles at JET

Analysis of Plasma EDGE Profiles at JET

M.N.A.Beurskens[1], E.Giovannozzi[2], J.Gunn[4], Y.Andrew[5], M.Brix[3], J-MChareau[4], K.Erents[5], C.Gowers[5], K.Günther[5], S.Jachmich[3], A.Kallenbach[8], A.Korotkov[5], E. de la Luna[6], P.Morgan[5], R.Prentice[5], M.Proschek[7], G.Saibene[9], W.Suttrop[8], J-MTravere[4], V.Tribaldos[6], M.Zerbini[2] and JET EFDA Contributors*

[1]FOM/Euratom instituut voor plasmafysica 'Rijnhuizen', Nieuwegein, Trilateral Euregio Cluster (TEC), The Netherland,
[2]Associazione Euratom-ENEA, V E Fermi 47, 00044 Frascati, Italy
[3]Forschungszentrum Jülich/Euratom, IPP, Jülich, TEC, Germany
[4]Association Euratom-CEA, Cadarache, F-13108 St. Paul-lez-Durance, France
[5]Euratom/UKAEA fusion Culham Science Centre, Abingdon, OX14 3EA, UK,
[6]Ciemat/Euratom, Madrid, Spain,
[7]TU Wien/Euratom, Vienna, Austria,
[8]Association Euratom-IPP, MPI fur Plasmaphysik, Garching, Germany
[9]EFDA Close Support Unit, Garching, MPI fur Plasmaphysik, Garching, Germany.
**See appendix of the paper by J.Pamela "Overview of recent JET results", Proceedings of the IAEA conference on Fusion Energy, Sorrento 2000*

Preprint of Paper to be submitted for publication in Proceedings of the EPS Conference,
(Madeira, Portugal 18-22 June 2001)

INTRODUCTION

JET plasma edge profiles from various diagnostics are combined to reconstruct the best edge n_e, T_e and p_e profile. Diagnosing edge profiles is essential in, for example, pedestal studies, edge gradient studies, stability analysis and input for edge current models. The comparison and combination of various diagnostics gives complementary information and yields a tool for validation: Edge LIDAR monitors T_e and n_e from the SOL up to the pedestal top. Core LIDAR gives an indication of the T_e and n_e pedestal top. ECE measures T_e from the top halfway down to the SOL. The Li beam gives a spatially resolved multiple n_e pedestal measurement. Interferometry indicates the pedestal top of n_e, is used as a n_e calibration source, and can be used to reconstruct ne profiles in swept plasmas. T_i measurements by CXS are important, but are not dealt with in this paper.

For comparison of the edge profiles, diagnostic lines of sight are carefully mapped onto the magnetic flux surfaces as calculated by the JET EFIT code (Fig. 1). The spatial mapping accuracy is + /- 2 cm at the last closed flux surface in the magnetic mid-plane. Table 1 shows the capabilities of the diagnostics used in this analysis. The indicated resolutions are given for the magnetic axis of the plasma and do not necessarily represent the individual diagnostic resolution. This is particularly true for the edge LIDAR diagnostic whose mid-plane resolution benefits from mapping the diagnostic line of sight from a region with large flux expansion to the magnetic axis where the flux surfaces are strongly compressed. The edge gradient measurement capabilities are presented via three examples of ELMy H-mode discharges that genuinely feature the steepest pressure gradients.

Table 1: resolution, penetration and limitation of edge diagnostics.

Diagnostic	Parameter	Resolution	Penetration	Comment
Edge LIDAR	T_e / n_e	2−5cm	5−15cm	Does not see pedestal
Edge LIDAR	T_e	1−2cm	Edge or core	Suffers from cut−off and shine−through
Edge LIDAR	n_e	1cm	5−10cm	Does not see pedestal if $n_e > 3.10^{19}$ m^{-3}
Edge LIDAR	n_e	(2cm) Abel inver.	20cm	Line integrated near edge

JG03.510-9c

1. TYPE I TO III ELM TRANSITION

High density ELMy H-mode discharges feature confinement loss at a certain density limit. At this limit the ELM behaviour changes from type I to Type III ELMs [1]. It is observed with the edge LIDAR diagnostic that in this transition the edge-pressure gradient becomes shallower. Figure 2 shows the ELM behaviour and the change of edge T_e, n_e and p_e gradient in the transition.

2. TRIANGULARITY AND EDGE PRESSURE GRADIENT.

At JET high triangularity means better confinement with higher edge pedestal pressure limits [2,3,4]. So far it has not been possible to compare edge gradients as a function of triangularity. A gas-scan experiment is performed in two shapes, (δ_{up}, δ_{low}) = (0.5, 0.45), (δ_{up}, δ_{low}) = (0.5, 0.3). Fig. 3 shows that gradient comparison with edge LIDAR is limited by the instrument resolution (Fig 3). Combining edge LIDAR and ECE yields pressure gradients of 320kPa/m and 250kPa/m for the subsequent cases (Fig 4 and 5). These gradients are still limited by the edge LIDAR resolution for ne and therefore they cannot be distinguished. In the future, optimising penetration will improve resolution (Fig. 3).

3. PRESSURE GRADIENT WITH LI-BEAM AND ECE.

For low density ELMy H-modes Li-beam measurements are possible. Under these conditions the higher spatial resolution of this diagnostic proves beneficial. An example is given of two discharges with different triangularity (Fig 6). The combined ECE, Li beam pressure profile shows gradients of 300-350 kPa/m.

CONCLUSIONS

True edge gradient measurements are observed up to the resolution limits of JET diagnostics. In practice this means that gradient measurements are possible in plasmas with degraded edge confinement (Type III ELMs). In type I ELMy H-modes, generally edge gradient measurements are limited by diagnostic resolution. Edge LIDAR is the only diagnostic with a direct edge pressure profile independent on EFIT equilibrium reconstruction for mapping purposes. Combining Li-beam and ECE yields edge pressure profiles with the best resolution possible at JET. Using these, electron pressure gradients of up to 300-350kPa/m have been measured. However, the mapping error of EFIT of +/-2cm in the midplane complicates the interpretation. In a new experiment for edge gradient measurement the plasma shape will be optimised for optimum access of Li beam and edge LIDAR. The edge LIDAR penetration can be tuned to yield higher resolution (1cm, Fig. 3) at the steep edge gradient region. Taking into account that edge T_e is limited by parallel transport, the Li beam and ECE measurements can be shifted with respect to edge LIDAR to match the separatrix [3]. And sweeping experiments enable profile reconstruction from interferometry.

REFERENCES

[1]. R.Sartori, this conference
[2]. G.Saibene, nucl. fusion, **39**, p1133, 1999
[3]. A.Kallenbach, this conference
[4] .G.Saibene, this conference.

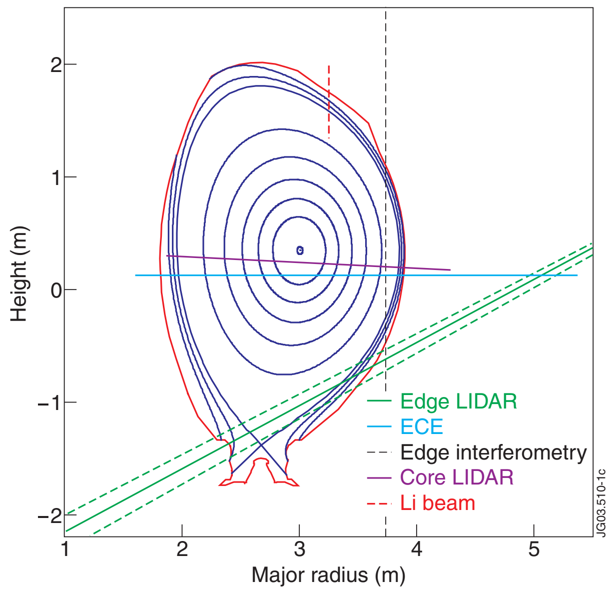

Figure 1: Diagnostic sight lines mapped onto flux surfaces.

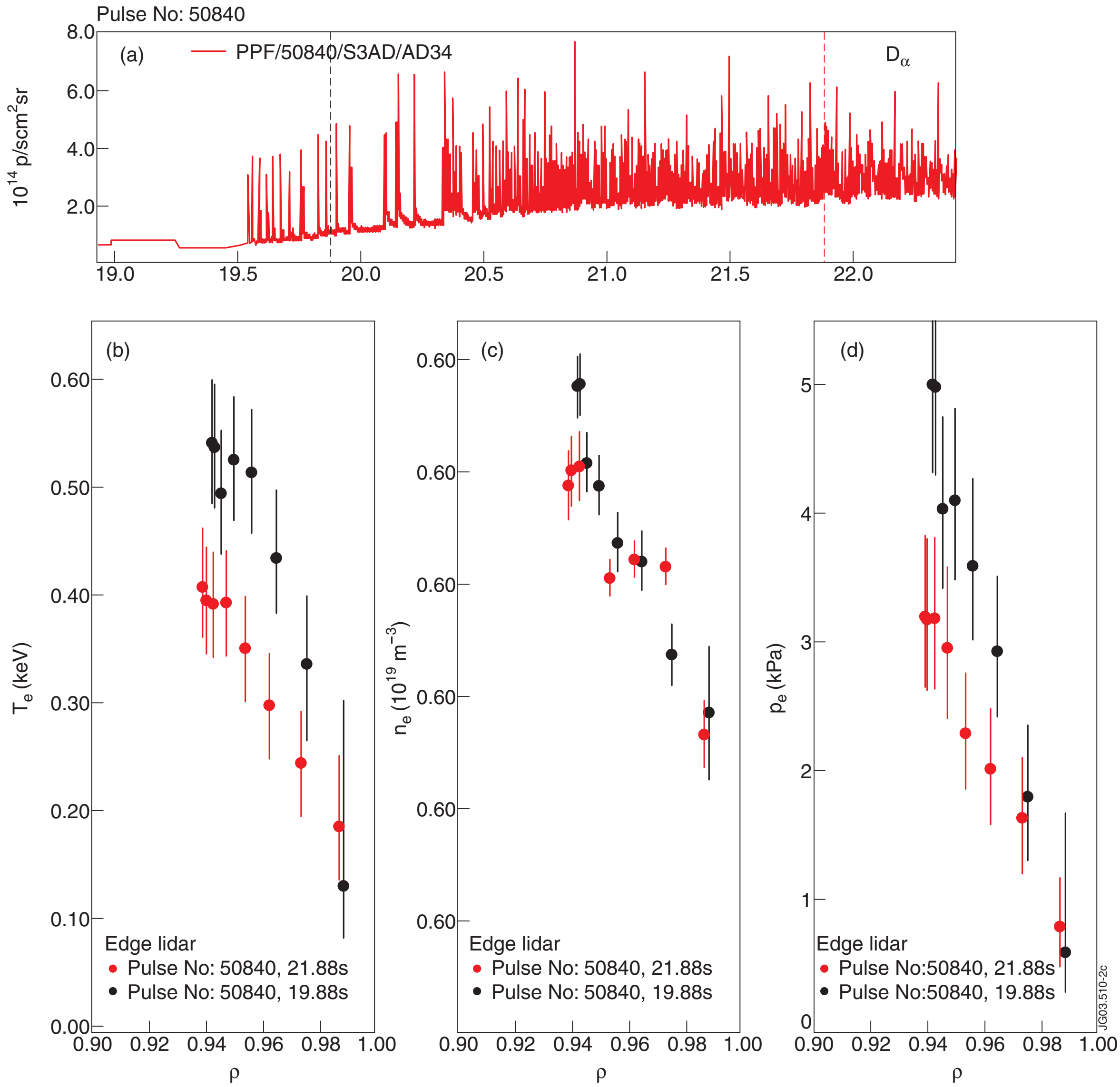

Figure 2: (a) D_α trace showing the ELM transition from Type I to Type III. Dashed lines indicate the edge LIDAR timing. (b, c, d) T_e, n_e and p_e profiles by edge LIDAR. Clearly the edge T_e and p_e gradients have dropped after the transition.

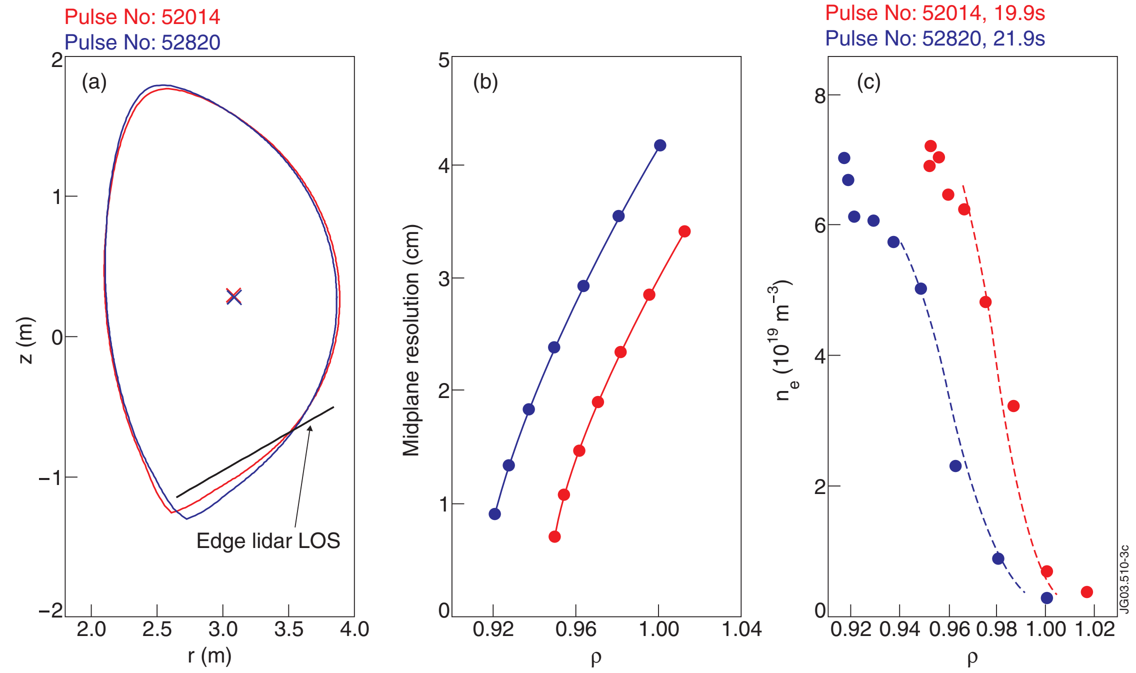

Figure 3: (a) Two shapes[(δ_{up}, δ_{low}) = (0.5, 0.45) = red, (δ_{up}, δ_{low}) = (0.5, 0.3) = blue] have different penetration for edge LIDAR and therefore (b) different resolution in the mid-plane. (c) Instrument resolution (drawn) limits gradient measurements in both cases.

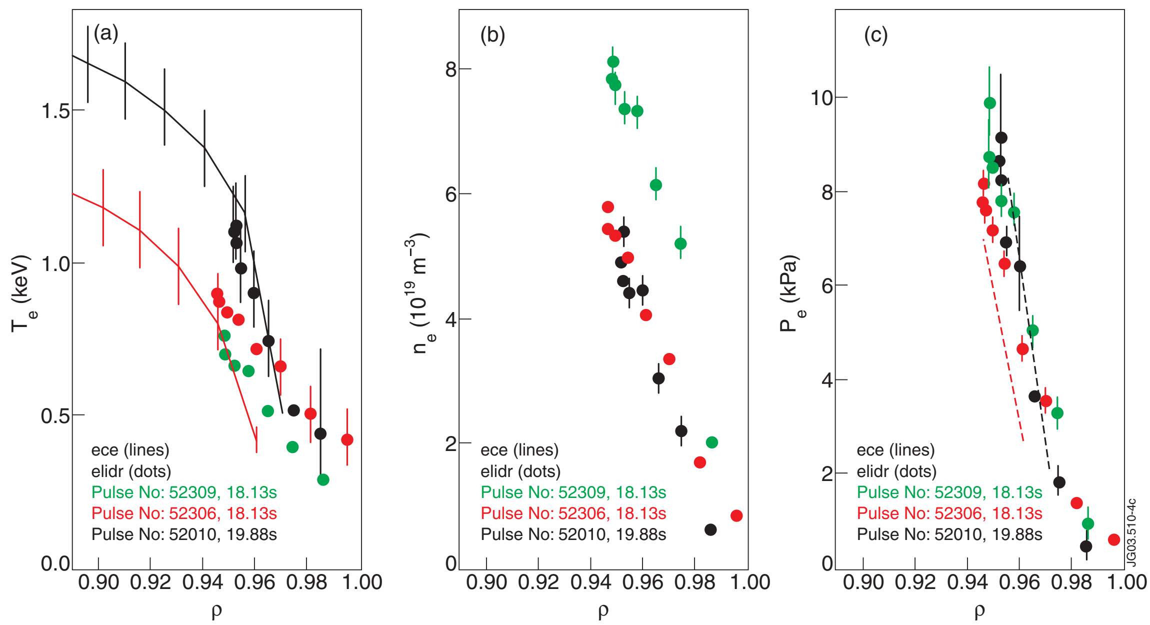

Figure 4: T_e, n_e and p_e profiles by edge LIDAR and ECE for (δ_{up}, δ_{low}) = (0.5, 0.45). p_e gradient does not vary within gas scan. Combined ECE and LIDAR yields highest p_e gradient.

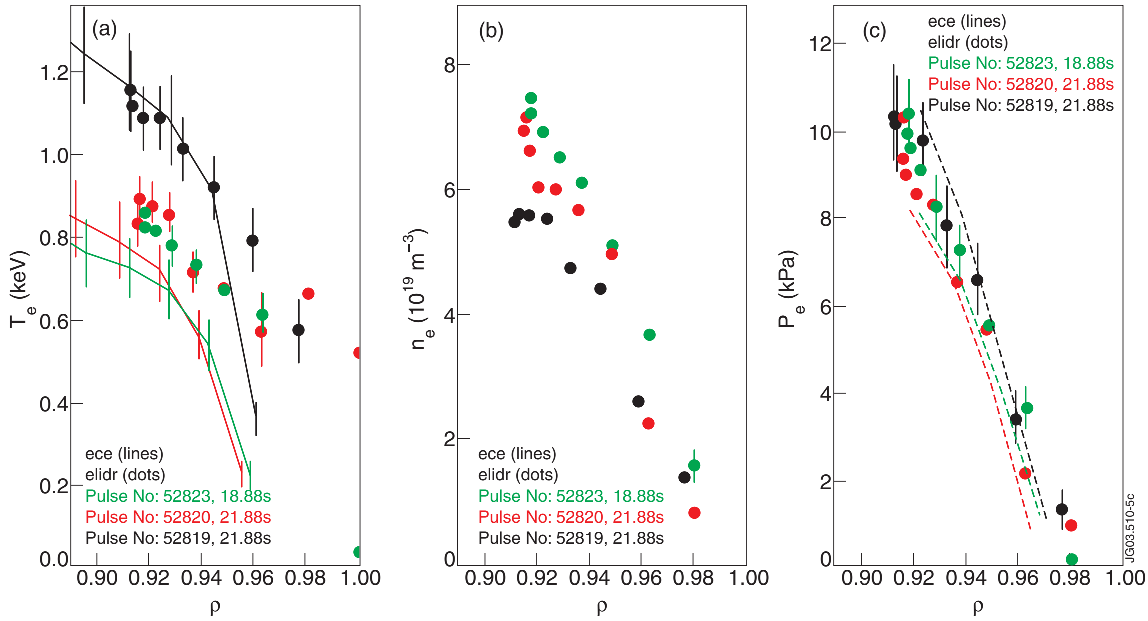

Figure 5: T_e, n_e and p_e profiles by edge LIDAR and ECE for (δ_{up}, δ_{low}) = (0.5, 0.3). p_e gradient does not vary within gas scan. Combined ECE and LIDAR yields highest pe gradient.

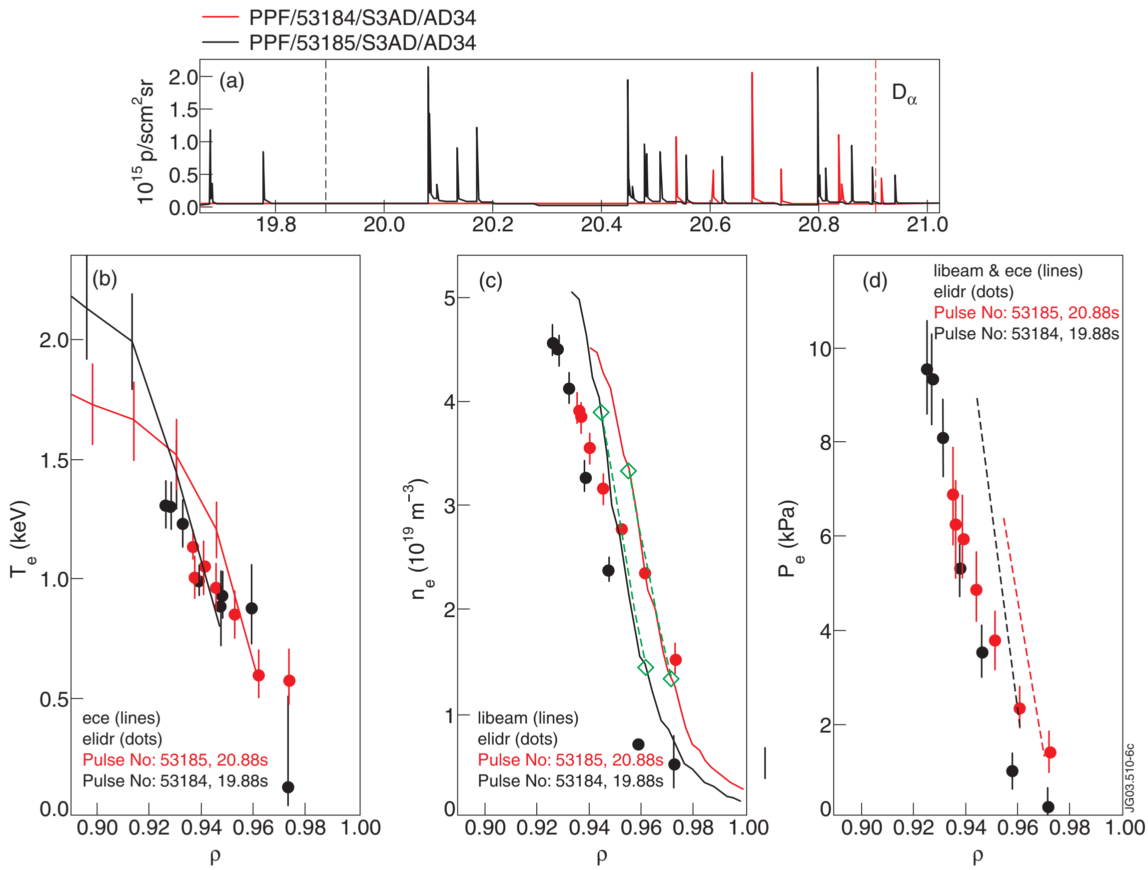

Figure 6: (a) The edge LIDAR measurements are taken away from an ELM for both cases. (b), (c) and (d) show T_e, n_e and p_e profiles by edge LIDAR, ECE and Li beam. Clearly ECE and Li beam measure steeper T_e, and n_e gradients resp. than edge LIDAR. For both plasmas the combined ECE, Li-beam pressure gradient therefore is steeper than in the edge LIDAR profile.